Synthesis and Investigation of Tin(II) Pyrophosphate $Sn_2P_2O_7$

Victoria V. Chernaya,[†] Alexander S. Mitiaev,[†] Pavel S. Chizhov,[†] Evgeny V. Dikarev,[‡] Roman V. Shpanchenko,*[,†] Evgeny V. Antipov,[†] Mikhail V. Korolenko,[†] and Pavel B. Fabritchnyi[†]

Department of Chemistry, Moscow State University, 119992 Moscow, Russia, and Department of Chemistry, University at Albany, State University of New York, Albany, New York 12222

Received September 8, 2004. Revised Manuscript Received November 3, 2004

The structural investigation of $Sn_2P_2O_7$ was carried out for the first time by means of single crystal and powder X-ray diffraction. The crystal structure of β-$Sn_2P_2O_7$ pyrophosphate was solved using single-crystal X-ray data at room temperature and at 93 K. At room temperature the structure (triclinic, $P\bar{1}$, $a = 5.2776(5)$ Å, $b = 11.5413(12)$ Å, $c = 11.6360(12)$ Å, $\alpha = 102.911(8)°$, $\beta = 99.303(8)°$, $\gamma = 98.899(8)°$, $V = 668.2(3)$ Å^3, $Z = 4$) contains the $[P_2O_7]^{4-}$ pyrophosphate groups oriented in mutually perpendicular directions with tin atoms situated in large structural interstices. This structure remains intact at low temperatures. The $Sn_2P_2O_7$ undergoes a reversible structural transition at 623 K found by thermal analysis which is accompanied by increase of the unit cell symmetry to monoclinic. The crystal structure of the high temperature α-$Sn_2P_2O_7$ form was solved using high-temperature powder diffraction data collected at 773 K. The structural motif of the high temperature form (monoclinic, $P2_1/n$, $a = 7.1765(4)$ Å, $b = 9.2874(6)$ Å, $c = 5.2968(4)$ Å, $\beta = 106.034(3)°$, $V = 339.30(5)$ Å^3, $Z = 2$) is closely related to the room temperature modification. The stereochemically active lone pairs of the tin atoms were localized with the ELF calculations for both polymorph modifications. In addition, the electronic state of tin was characterized using ^{119}Sn Mössbauer spectroscopy.

Introduction

Crystalline and amorphous tin pyrophosphates $Sn_2P_2O_7$ have recently received significant attention as prospective new negative electrode materials for lithium batteries. Several groups of authors have investigated the lithium insertion in this material as well as its cyclic characteristics.[1−4] In the range of potentials 0−1.2 V (vs Li^+/Li), amorphous and crystalline $Sn_2P_2O_7$ were found to deliver reversible specific capacities of 520 and 400 mAh/g, respectively.[2] Despite the commercial availability of $Sn_2P_2O_7$ (98% purity reagent by Aldrich), there is no structural, or even reliable diffraction, information about this phase. The knowledge of the crystal structure of the title compound is important for continuing the search for better materials, as well as for understanding why certain structures and compositions of tin-based materials are providing useful performance as negative electrodes in lithium-ion cells.

In a number of studies, IR,[2−4] Mössbauer[5,6] and differential thermal analysis[7] data have been used for characterization of the $Sn_2P_2O_7$ pyrophosphate. On the other hand, the X-ray diffraction data for this compound are very scant and inconsistent. Two completely different data sets reported earlier[5,8] were not indexed. The X-ray pattern of $Sn_2P_2O_7$ presented by Behm et al.[1] does not correspond to those obtained by other authors.[2]

In this work, we present the results of the structural characterization and investigation of tin(II) pyrophosphate $Sn_2P_2O_7$ using both single crystal and powder X-ray diffraction data at different temperatures, as well as the results obtained for the same material by means of DTA and Mössbauer spectroscopy.

Experimental Section

The bulk sample of pure $Sn_2P_2O_7$ was obtained by heating a stoichiometric mixture of SnO and $NH_4H_2PO_4$ in dynamic vacuum or in argon flow at 820 K for 24 h. $Sn_2P_2O_7$ melts at about 870 K forming an amorphous glass. Therefore, to obtain the single crystals for X-ray study the sample synthesized at 820 K was further annealed at 850 K in a sealed, evacuated quartz ampule for one month.

X-ray powder diffraction (XRPD) data at room temperature (RT) were collected on a STOE diffractometer ($CuK\alpha_1$ radiation, Ge monochromator, linear PSD). High-temperature (HT) powder diffraction experiment was performed at 773 K with a ThermoARL X'TRA diffractometer (Cu Kα radiation, Si detector). The data collection for single-crystal structure refinement at RT was done using a CAD4 diffractometer. Low-temperature (LT) single-crystal experiment was performed on a Bruker APEX CCD X-ray diffractometer equipped with a Bruker CRYO-FLEX low-temper-

* To whom correspondence should be addressed. E-mail: shpanchenko@icr.chem.msu.ru.

[†] Moscow State University.

[‡] University at Albany, SUNY.

(1) Behm, M.; Irvine, J. T. S. *Electrochim. Acta* **2002**, *47*, 1727−1738.
(2) Xiao, Y. W.; Lee, J. Y.; Yu, A. S.; Liu, Z. L. *J. Electrochem. Soc.* **1999**, *146*, 3623−3629.
(3) Wan, K.; Li, S. F. Y.; Gao, Z.; Siow, K. S. *J. Power Sources* **1998**, *75*, 9−12.
(4) Lee, J. Y.; Xiao, Y.; Liu, Z. *Solid State Ionics* **2000**, *133*, 25−35.
(5) Lees, J. K.; Flinn, P. A. *J. Chem. Phys.* **1968**, *48*, 882−889.
(6) . P. A. Flinn. In *Mössbauer Isomer Shifts*; Shenoy, G. K.; Wagner, F. E., Eds.; North-Holland: Amsterdam, 1978; p 593.
(7) Shitova, V. I. Popova, V. F.; Grabovenko, L. Yu.; Kuchaeva, S. K.; Grebenschikov, R. G. *Zh. Prikl. Khimii (Russ.)* **1996**, *69*, 1946−1950.
(8) Chernorukov, N. G.; Sibrina, G. F.; Zabelin, A. I. *Zh. Neorg. Khimii (Russ.)* **1979**, *24*, 2333−2336.

10.1021/cm048463h CCC: $30.25
Published on Web 12/31/2004

Table 1. Data Collection and Structural Parameters for $Sn_2P_2O_7$

	β-$Sn_2P_2O_7$		α-$Sn_2P_2O_7$
temperature, K	293	93	773
formula weight		411.36	
crystal system		triclinic	monoclinic
space group (No.)		$P\bar{1}$ (2)	$P2_1/n$ (14)
a (Å)	5.2776(5)	5.2570(6)	7.1765(4)
b (Å)	11.5413(12)	11.4464(14)	9.2874(6)
c (Å)	11.6360(12)	11.5610(14)	5.2968(4)
α (deg)	102.911(8)	101.616(2)	
β (deg)	99.303(8)	99.158(2)	106.034(3)
γ (deg)	98.899(8)	98.701(2)	
V (Å^3)	668.2(3)	660.54(14)	339.30(5)
Z		4	2
D_{calc} (g·cm^{-3})	4.088	4.135	4.026
radiation, wavelength (Å)		Mo Kα, 0.71073	Cu Kα, 1.54184
μ (cm^{-1})	7.942	8.034	6.523
color		colorless	pale gray
diffractometer	CAD4	Bruker APEX CCD	X'TRA ThermoARL
crystal size (mm^3)	0.2 × 0.12 × 0.07	0.05 × 0.03 × 0.01	
no. of measured reflections	6926	5697	
no. of independent reflections ($I \geq 3\sigma$)	5155	2526	
2θ range (°)	4−72	4−56	16−66
Range of h, k, l	$0 \rightarrow h \rightarrow 8$	$-6 \rightarrow h \rightarrow 6$	$0 \rightarrow h \rightarrow 5$
	$-19 \rightarrow k \rightarrow 18$	$-14 \rightarrow k \rightarrow 15$	$0 \rightarrow k \rightarrow 6$
	$-19 \rightarrow l \rightarrow 18$	$-15 \rightarrow l \rightarrow 15$	$-3 \rightarrow l \rightarrow 3$
refinement		on F	full profile
program used		JANA2000	GSAS
$R/R_w(I > 3\sigma(I))$ or R_P/R_{wP}	0.036/0.041	0.053/0.063	0.104/0.135
GOF/wGOF or GOF/χ^2	1.86/1.69	3.74/3.81	1.14/1.29
no. of refined parameters	200	199	46
extinction B-C type 1 Gaussian iso	0.093(2)		
weighting scheme, $(\Delta/\sigma)_{max}$		unit	
$\Delta\rho_{max}$ (e/Å^3) positive/negative	1.70/−1.49	3.78/−2.18	

ature attachment. Single-crystal structure computations were carried out using the CSD program package,[9] and the final refinement was made with the JANA2000 program.[10]

The bonding character in the structure was analyzed using the electron localization function (ELF).[11] First, the calculations were performed for both RT and HT modifications of tin pyrophosphate using the LMTO 4.7 program package.[12] The Barth−Hedin exchange-correlation potential was used in DFT calculations performed for 12 k-points in the irreducible Brillouin zone (IBZ) for RT (triclinic) phase and for 40 k-points in IBZ for HT (monoclinic) phase. The calculations clearly show that $Sn_2P_2O_7$ is an insulator in any modification. The ELF distribution was obtained using the intrinsic program procedure.

Thermal analysis was performed on NETZSCH STA 449C instrument in purified argon flow in the 290−970 K temperature range. LT scanning calorimetry experiment was carried out with NETZSCH DSC 204 Phoenix device at the cooling rate of 10 K/min.

The ^{119}Sn spectra were recorded using a conventional Mössbauer spectrometer operating in constant acceleration mode with a $Ca^{119m}SnO_3$ source kept at RT. The absorbers for Mössbauer measurements were prepared by thoroughly mixing the appropriate amounts of synthesized polycrystalline $Sn_2P_2O_7$ with Al_2O_3 powder and packing the mixture in a double cuvette plastic cell. The thickness of the absorber was 13.7 mg of $Sn_2P_2O_7$ per cm^2 at 295 K and 7.1 mg/cm^2 at 80 K. All isomer shift values are reported with respect to $CaSnO_3$ reference absorber at 295 K. The spectra were analyzed using standard computer techniques.

(9) Akselrud, L. G.; Zavalij, P. Y.; Grin, Yu. N.; Pecharsky, V. K.; Baumgartner, B.; Wolfel, E. *Mater. Sci. Forum* **1993**, *133*−*136*, 335.
(10) Petriček, V.; Dusek, M. *Jana2000. Structure Determination Software Programs*; Institute of Physics, Praha, Czech Republic.
(11) Savin, A.; Jepsen, O.; Flad, J.; Andersen, O. K.; Preuss, H.; von Schnering, H. G. *Ang. Chem. Int. Ed. Engl.* **1992**, *31*, 187−188.
(12) Krier, G.; Jepsen, O.; Burkhart, A.; Andersen, O. K. *The TB-LMTO-ASA Program*; Stuttgart, 1995.

Results

Crystal Structure of β-$Sn_2P_2O_7$ at Room and Low Temperature. Diffraction data of colorless single crystal of $Sn_2P_2O_7$ at RT were indexed in triclinic symmetry with the unit cell parameters $a = 5.2776(5)$ Å, $b = 11.5413(12)$ Å, $c = 11.6360(12)$ Å, $\alpha = 102.911(8)°$, $\beta = 99.303(8)°$, $\gamma = 98.899(8)°$. Positions of the tin atoms were obtained from direct methods; the coordinates of the P and O atoms were determined by sequential series of Fourier and difference Fourier syntheses. The final refinement was carried out in the $P\bar{1}$ space group with an anisotropic approximation for displacement parameters for all atoms and resulted in R/R_w values of 0.036/0.041. Crystallographic data and experimental conditions are listed in Table 1 and the atomic and isotropic displacement parameters are given in Table 2. Main interatomic distances and angles in the structure are listed in Table 3.

Two projections of the $Sn_2P_2O_7$ crystal structure are shown in Figure 1. The structure contains isolated $[P_2O_7]^{-4}$ pyro-

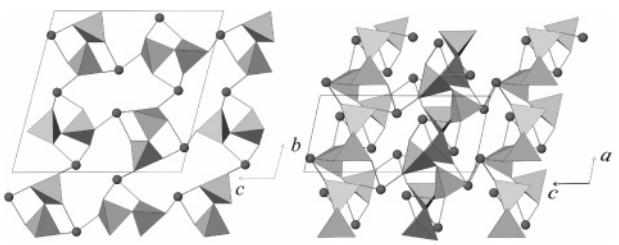

Figure 1. Projections of the β-$Sn_2P_2O_7$ structure onto (011) (left) and (101) (right) planes.

phosphate groups oriented in two nearly perpendicular directions. The tin atoms are located between each pair of

Table 2. Atomic Positional and Isotropic Displacement Parameters for β-$Sn_2P_2O_7$ at 293 K

atom	*x*	*y*	*z*	*U*
Sn(1)	0.27139(7)	0.50457(3)	0.14256(3)	0.01487(9)
Sn(2)	0.17735(7)	−0.15098(4)	−0.01932(3)	0.01607(9)
Sn(3)	0.69283(7)	−0.04478(4)	0.36751(4)	0.01730(10)
Sn(4)	0.23083(7)	0.36723(4)	0.47328(3)	0.01600(9)
P(1)	0.2856(3)	0.12027(12)	0.25155(12)	0.0120(3)
P(2)	0.6910(2)	0.33244(12)	0.25542(12)	0.0115(3)
P(3)	0.1857(3)	−0.26956(13)	0.35521(12)	0.0130(3)
P(4)	0.7946(3)	−0.26788(13)	0.14624(12)	0.0132(3)
O(1)	0.1438(9)	−0.3229(4)	−0.1599(4)	0.0200(12)
O(2)	0.6463(9)	−0.1752(5)	0.2002(4)	0.0262(14)
O(3)	0.8524(9)	−0.2539(5)	0.0254(4)	0.0212(12)
O(4)	0.8518(10)	0.3805(5)	0.3821(4)	0.0290(15)
O(5)	0.1745(9)	0.1951(4)	0.3470(4)	0.0226(13)
O(6)	0.4720(9)	0.4006(4)	0.2394(4)	0.0210(12)
O(7)	0.3567(9)	0.0067(4)	0.2806(5)	0.0223(13)
O(8)	0.0828(7)	−0.2416(4)	0.2283(4)	0.0160(10)
O(9)	0.8959(12)	−0.0863(5)	−0.1285(4)	0.0329(17)
O(10)	0.0357(9)	0.2663(5)	0.5777(4)	0.0233(13)
O(11)	0.4184(9)	−0.1667(5)	0.4196(4)	0.0243(13)
O(12)	0.6676(10)	0.6034(5)	0.1399(5)	0.0284(15)
O(13)	0.2682(11)	0.6088(4)	0.3237(4)	0.0261(15)
O(14)	0.5592(10)	0.1934(4)	0.2408(6)	0.0324(18)

$[P_2O_7]^{4-}$ units that form a nearly square net. Due to such orientation, large cavities appear in the structure along the *a*-axis.

There are two types of P−O distances within PO_4 tetrahedra. The distances to bridging O atoms (1.594(6) − 1.608(5) Å are considerably longer than those to terminal O atoms (1.504(5) − 1.527(4) Å). The pyrophosphate groups are distorted and have no inversion center at the bridging O(8) and O(14) atoms as is typically the case for most pyrophosphate structures. Therefore, the P(3)−O(8)−P(4) and P(1)−O(14)−P(2) angles are 131.5(3)° and 137.1(4)°, respectively. Tin atoms have 3-fold coordination that is usual for Sn^{2+} cation having a sterically active lone pair. The Sn−O distances are in the range of 2.108−2.234 Å typical for tin(II) oxides. However, if we take into account the second coordination sphere, the Sn(1) atom noticeably differs from the three others. The Sn(1) atom has a fourth oxygen atom at a distance of 2.855(5) Å, whereas the other tin atoms have fourth oxygen neighbors at distances of longer than 3.0 Å. A visualization of the ELF results (Figure 2) clearly shows the presence and the localization of the lone pair on the tin atoms. Every tin atom has pyramidal coordination of three oxygen atoms with lone pairs completing a coordination arrangement to pseudo-tetrahedral one.

The crystal structure of $Sn_2P_2O_7$ determined at 93 K (Tables 1) remains almost unchanged compared to that at RT. The Sn−O and P−O distances are only slightly changed without any systematic correlations. The sole exception is the Sn(1)−O(1) separation which is slightly reduced to 2.809(10) Å (2.855(5) Å at 293 K). The absence of structural transformations down to 80 K was also confirmed by LT calorimetry.

Mössbauer Spectroscopy Characterization. All previous Mössbauer investigations of $Sn_2P_2O_7$ indicated a presence of tetravalent tin in the samples although neither XRPD nor optical measurements revealed SnO_2 as an individual phase.[7] Thus, it was not clear whether the stannic ions were located in the pyrophosphate lattice. The structure solution unambiguously demonstrated that all four Sn positions in the

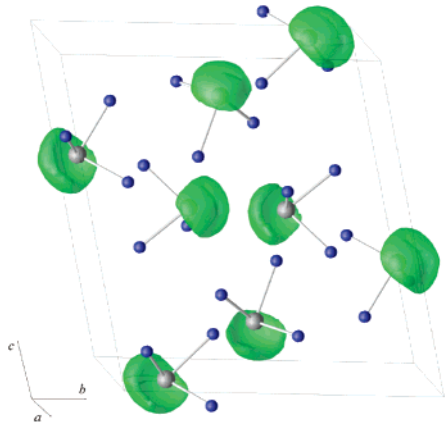

Figure 2. Coordination arrangement of tin atoms in the β-$Sn_2P_2O_7$ structure. Lone electron pairs on the Sn atoms are localized by the ELF calculations ($\eta = 0.85$).

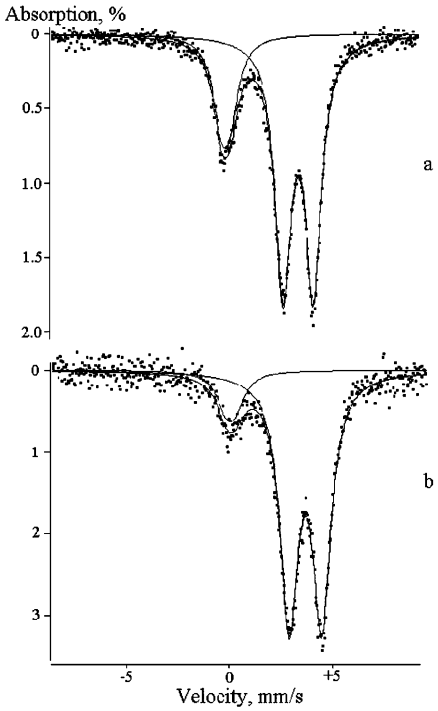

Figure 3. Mössbauer spectra of tin pyrophosphate recorded at 295 K (a) and 80 K (b).

structure are occupied by divalent tin only. To elucidate the earlier results $Sn_2P_2O_7$ material was characterized by means of Mössbauer spectroscopy. For this purpose we prepared a single-phase powdered sample of $Sn_2P_2O_7$, its XRPD pattern is shown in Figure 6a.

The spectrum recorded at 295 K (Figure 3a) consists of a well-resolved doublet situated at positive velocities and an unresolved doublet in the center part of the pattern. The observed values of isomer shift ($\delta_1 = 3.37 \pm 0.02$ mm/s) and quadrupole splitting ($\Delta_1 = 1.47 \pm 0.03$ mm/s) of the former doublet are characteristic of the +2 valence state, while the value of Δ_1 is somewhat lower than that reported previously for $Sn_2P_2O_7$ ($\delta = 3.35$ mm/s, $\Delta = 1.61$ mm/s).[5] The parameters of the latter doublet ($\delta_2 = -0.15 \pm 0.02$ mm/s, $\Delta_2 = 0.42 \pm 0.03$ mm/s), that are characteristic of Sn^{4+} ions, show that the material used for Mössbauer measurements was contaminated to a certain extent with oxidized tin species. The high value of Δ_1 implies the

Table 3. Major Interatomic Distances (Å) and Angles (deg) for β-$Sn_2P_2O_7$ at 293 K

Sn(1)−O(1)	2.855(5)	P(1)−O(5)	1.504(5)	O(6)−Sn(1)−O(12)	85.9(2)
Sn(1)−O(6)	2.108(5)	P(1)−O(7)	1.511(5)	O(6)−Sn(1)−O(13)	82.3(2)
Sn(1)−O(12)	2.230(5)	P(1)−O(9)	1.520(5)	O(13)−Sn(1)−O(12)	94.2(2)
Sn(1)−O(13)	2.185(5)	P(1)−O(14)	1.594(6)	O(1)−Sn(1)−O(12)	162.2(2)
				O(1)−Sn(1)−O(13)	89.8(2)
Sn(2)−O(1)	2.234(4)	P(2)−O(1)	1.515(5)	O(1)−Sn(2)−O(3)	82.7(2)
Sn(2)−O(3)	2.135(5)	P(2)−O(4)	1.512(5)	O(1)−Sn(2)−O(9)	93.6(2)
Sn(2)−O(9)	2.129(6)	P(2)−O(6)	1.505(5)	O(3)−Sn(2)−O(9)	86.5(2)
		P(2)−O(14)	1.607(5)	O(2)−Sn(3)−O(7)	84.4(2)
Sn(3)−O(2)	2.131(5)			O(2)−Sn(3)−O(11)	89.2(2)
Sn(3)−O(7)	2.130(5)	P(3)−O(8)	1.608(5)	O(7)−Sn(3)−O(11)	84.8(2)
Sn(3)−O(11)	2.117(5)	P(3)−O(10)	1.507(5)	O(4)−Sn(4)−O(5)	86.3(2)
		P(3)−O(11)	1.527(4)	O(4)−Sn(4)−O(10)	88.1(2)
Sn(4)−O(4)	2.152(5)	P(3)−O(13)	1.518(6)	O(5)−Sn(4)−O(10)	84.5(2)
Sn(4)−O(5)	2.137(4)			P(3)−O(8)−P(4)	131.5(3)
Sn(4)−O(10)	2.135(6)	P(4)−O(2)	1.506(6)	P(1)−O(14)−P(2)	137.1(4)
		P(4)−O(3)	1.523(5)		
		P(4)−O(8)	1.605(4)		
		P(4)−O(12)	1.512(6)		

Table 4. Mössbauer Parameters for the Sample of Tin Pyrophosphate

temp. K	tin valence state	isomer shift, ±0.02 mm/s	quadrupole splitting, ±0.03 mm/s	full width at half-maximum, ±0.03 mm/s	spectral contribution, ±3%
295	II	$\delta_1 = 3.37$	$\Delta_1 = 1.47$	0.92	78
	IV	$\delta_2 = -0.15$	$\Delta_2 = 0.44$	1.02	22
80	II	$\delta_1 = 3.45$	$\Delta_1 = 1.57$	1.02	88
	IV	$\delta_2 = -0.10$	$\Delta_2 = 0.45$	1.02	12

presence of a sterically active lone electron pair, which is in agreement with low coordination number of the Sn^{2+} ions as was revealed by crystal structure solution. However, the observed Sn^{2+} doublet does not allow the extraction of individual contributions which could be assigned to different Sn^{2+} positions. This implies that tin valence electron hybridization (which is mainly responsible for the electric field gradient (EFG) probed by $^{119}Sn^{2+}$ nuclei) is not noticeably affected by the small differences in the local arrangement of the concerned crystallographic positions. In fact, the coordination arrangement for three of the four available Sn^{2+} sites is the same (CN = 3). Although the coordination sphere for the fourth Sn(1) atom involves four oxygen atoms, the Sn(1)−O(1) distance is much longer (2.855(5) Å) than the three others. This fact allows us to consider the effective coordination number for Sn(1) as close to 3. According to Flinn,[6] the observed value of δ_1 corresponds to the $5s^{1.4}5p^{0.6}$ hybridization, which could be assigned to any Sn^{2+} site in the structure of $Sn_2P_2O_7$.

The spectrum recorded at 80 K (Figure 3b) shows only small changes in both δ and Δ values (Table 4). In fact the structure rearrangement, which was displayed between 295 and 93 K by structure refinement, seems to produce no detectable specific effect on the ^{119}Sn hyperfine parameters. At 80 K, the slight increase in isomer shift can be accounted for by the second-order Doppler shift and that in quadrupole splitting can be accounted for by the regular minor evolution of the EFG term associated with neighboring ionic charges due to the contraction of the unit cell upon lowering the temperature. Finally, a lower contribution of the Sn^{4+} spectral component at 80 K is certainly due to a weaker temperature dependence of the Mössbauer recoil-free fraction for the Sn^{4+} cation as compared to that for Sn^{2+} one. The ratio of the Sn^{4+} to Sn^{2+} spectral contributions determined at 80 K allows us to evaluate the content of the Sn^{4+} species as ca. 10 at. %. The fact that XRPD has revealed no impurity in the studied sample prompts us to suggest that the Sn^{4+}-containing species are present as noncrystalline segregations. It is noteworthy that the Sn^{4+} doublet is characterized by a negative isomer shift which is rather unusual for this cation in crystalline oxide compounds. However, similar negative δ values have been earlier reported for some tin-oxide glasses which were believed to allow the formation of highly ionic Sn−O bonds.[13] Thus it seems likely that in the studied sample the Sn^{4+} species are present as vitreous segregations.

DTA Study and Crystal Structure of α-$Sn_2P_2O_7$. Thermal behavior of $Sn_2P_2O_7$ was investigated at both low and high temperatures. No evidence for structural transition was detected on going from RT to 100 K. This result is in agreement with the LT structure analysis and Mössbauer spectroscopy data. As mentioned before, the $Sn_2P_2O_7$ melts at ca. 873 K forming an X-ray amorphous glass. Figure 4a shows heating (3) and cooling (4) curves recorded near the melting point at a rate of 2 K/min. No crystallization peak appears on the cooling curve. Neither gain nor loss of the sample mass was detected. The X-ray pattern of the cooled sample is shown in Figure 5.

$Sn_2P_2O_7$ undergoes a reversible phase transition at 623 K. The relevant DTA curves (5 K/min) are shown in Figure 4b. We were unable to quench the HT form of $Sn_2P_2O_7$, and only the LT modification appeared on the XRPD patterns of the quenched samples. For this reason the HT powder diffraction experiment was performed at 773 K in a purified argon flow. The XRPD patterns for the HT α- and LT β-$Sn_2P_2O_7$ polymorphs are presented in Figure 6. The X-ray spectrum of β-$Sn_2P_2O_7$ is somewhat similar to that described by Shitova et al.[7] as well as by Behm and Irvine.[1] The latter pattern, however, contains strong peaks of another phase. The analysis of peak and intensity distribution for the HT and LT patterns indicates close relation between the two

(13) Mitrofanov, K. P.; Sidorov, T. A. *Sov. Phys. Solid State* **1967**, *9*, 963.

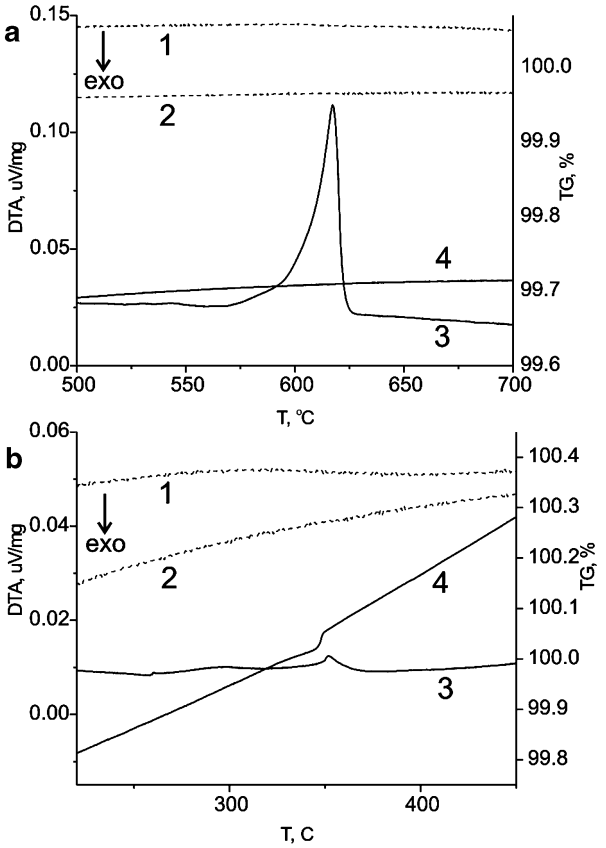

Figure 4. DTA data showing melting (a) and reversible phase transition (b) of the $Sn_2P_2O_7$ sample. In both figures the curves are numbered as 1, TG heating; 2, TG cooling; 3, DTA heating; 4, DTA cooling.

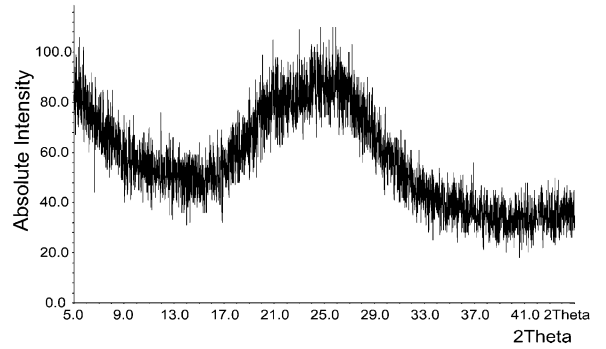

Figure 5. XRPD pattern of the $Sn_2P_2O_7$ sample taken after DTA experiment.

structures. The X-ray pattern of α-$Sn_2P_2O_7$ was indexed by the TREOR program[14] in monoclinic symmetry with the lattice parameters of $a = 7.177(2)$ Å, $b = 9.286(2)$ Å, $c = 5.298(1)$ Å, $\beta = 106.05(1)°$, and $V = 339.3(2)$ Å^3. The cell volume, which is half of that for the LT form suggests $Z = 2$ for the HT structure. The systematic extinctions, $h0l$: $h + l = 2n$ and $0k0$: $k = 2n$, clearly deduced from the XRPD pattern, unambiguously indicate the $P2_1/n$ space group.

The structural model for α-$Sn_2P_2O_7$ was obtained with the FOX program[15] based on the unit cell parameters and the space group determined earlier. Independent phosphate tetrahedra (as rigid bodies) and Sn atoms were randomly

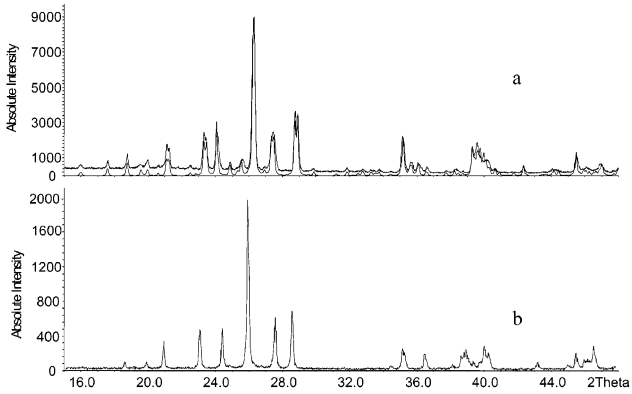

Figure 6. XRPD patterns of (a) LT β-$Sn_2P_2O_7$ (experimental and calculated from the single-crystal data curves are shown) and (b) HT α-$Sn_2P_2O_7$.

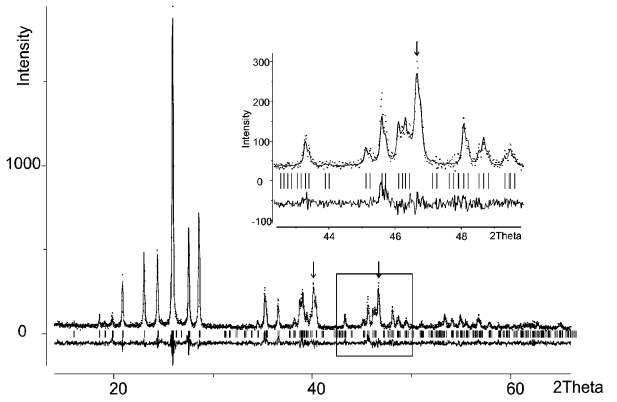

Figure 7. Observed, calculated, and difference X-ray patterns of α-$Sn_2P_2O_7$. Experimental data were collected at 773 K. Peaks from Pt sample holder are marked with arrows.

Table 5. Atomic Positional Parameters for α-$Sn_2P_2O_7$ (773 K)

atom	position	*x*	*y*	*z*	*U*
Sn	4e	0.1539(8)	0.6215(5)	0.7945(10)	0.025[a]
P	4e	0.908(3)	0.113(2)	0.776(3)	0.025[a]
O(1)	2a	0	0	0	0.025[a]
O(2)	4e	0.737(5)	0.031(3)	0.650(6)	0.025[a]
O(3)	4e	0.824(5)	0.184(3)	0.965(6)	0.025[a]
O(4)	4e	0.064(5)	0.162(3)	0.700(6)	0.025[a]

[a] Fixed.

distributed in the unit cell. During the computations two pairs of independent PO_4 tetrahedra formed P_2O_7 pyrogroups. The final Rietveld refinement was carried out with the GSAS program.[16] Because of low statistics for high temperature experiment, only the data in a range of 16−66° 2θ were used for computations. The displacement parameters for all atoms were not refined and were fixed at 0.025 Å^2. The observed, difference, and calculated patterns for α-$Sn_2P_2O_7$ are shown in Figure 7. Experimental parameters and crystal data are listed in Table 1. Atomic positions and main interatomic distances in the structure are given in Tables 5 and 6, respectively.

Three projections of the α-$Sn_2P_2O_7$ crystal structure are shown in Figure 8. The structure contains isolated $[P_2O_7]^{4-}$ pyrophosphate groups with the Sn atoms situated in the structural interstices. There are also two types of P−O

(14) Werner, P.-E.; Eriksson, L.; Westdahl, M. *J. Appl. Crystallogr.* **1985**, *18*, 367−370.
(15) Favre-Nicolin, V.; R. Černý, *J. Appl. Crystallogr.* **2002**, *35*, 734−743.
(16) (a) Larson, A. C.; Von Dreele, R. B. *General Structure Analysis System (GSAS)*; Los Alamos National Laboratory Report LAUR 86-748; Los Alamos, New Mexico, 1994. (b) Toby, B. H. *J. Appl. Crystallogr.* **2001**, *34*, 210−213.

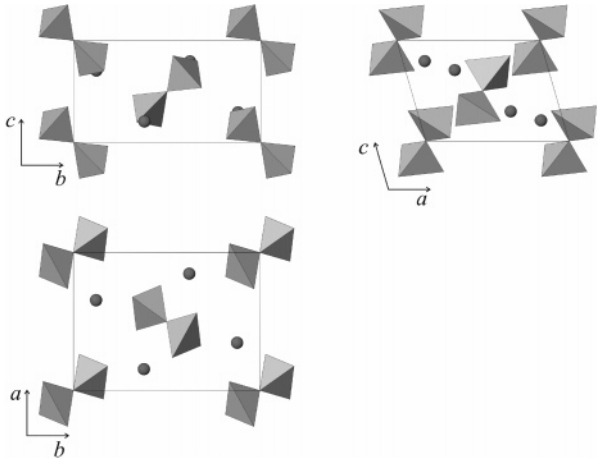

Figure 8. Projections of the α-$Sn_2P_2O_7$ structure onto three planes.

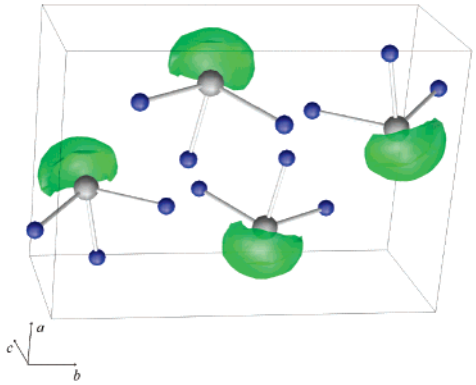

Figure 9. Coordination arrangement of tin atoms in the α-$Sn_2P_2O_7$ structure. Lone electron pairs of the Sn atoms are localized by the ELF calculations ($\eta = 0.85$).

distances as is usually observed for the pyrophosphate group. Three short P−O separations of about 1.42(2) and one longer bond of 1.58(2) Å to the bridging O(1) atom are found for the anion. The O(1) atom is situated on the inversion center; therefore, both PO_4 tetrahedra in the $[P_2O_7]$ group are equivalent and the P−O(1)−P angle is equal to 180.0° in contrast to those in β-$Sn_2P_2O_7$. The tin atom has three oxygen

Table 6. Major Interatomic Distances (Å) and Angles (deg) for α-$Sn_2P_2O_7$ (773 K)

Sn−O(2)	2.30(3)	P−O(1)	1.58(2)
Sn−O(3)	2.20(3)	P−O(2)	1.44(3)
Sn−O(4)	2.05(3)	P−O(3)	1.46(3)
O(2)−Sn-O(3)	94.1(9)	P−O(4)	1.37(3)
O(2)−Sn-O(4)	93.9(11)	P−O(1)−P	180.0
O(3)−Sn-O(4)	85.8(10)		

neighbors with Sn−O distances of 2.30(3), 2.20(3), and 2.05(3) Å. It is worth noting that the low experimental data statistics and, consequently, low precision in atomic position determination allow us to discuss an average structural model only, but not the details in bond distances. Figure 9 shows the coordination of the tin atoms in the structure of α-$Sn_2P_2O_7$. A visualization of the ELF results revealed a strong localization of the lone electron pair on the tin atoms similar to that found for the β-$Sn_2P_2O_7$ structure.

The ^{119}Sn spectrum was recorded at 650 K in argon atmosphere, using a thin-window quartz sample cell. Unfortunately, the drastic decrease in the relative contribution of Sn^{2+} component as compared to that of Sn^{4+} did not allow the impact of the structure transition on the Mössbauer parameters of the stannous tin to be examined.

Discussion

The structural features of $Sn_2P_2O_7$ are mostly defined by a crystallochemistry of the Sn^{2+} ion having a sterically active lone electron pair. In fact, the coordination of tin atoms in such structures is close to tetrahedral and can be written as SnO_3E (where E stands for a lone pair). A lone electron pair occupies a considerable part of the unit cell volume and, therefore, the structure must be adjusted to include such an extra space. In the structure of $Sn_2P_2O_7$, such an adjustment is achieved probably by almost perpendicular location of the P_2O_7 groups, whereas in most of the M_2^{II} P_2O_7 structures, the pyrophosphate groups are oriented parallel to each other. Apparently, the lone pairs of the tin atoms are directed into large structural interstices as shown in Figures 2 and 9. It

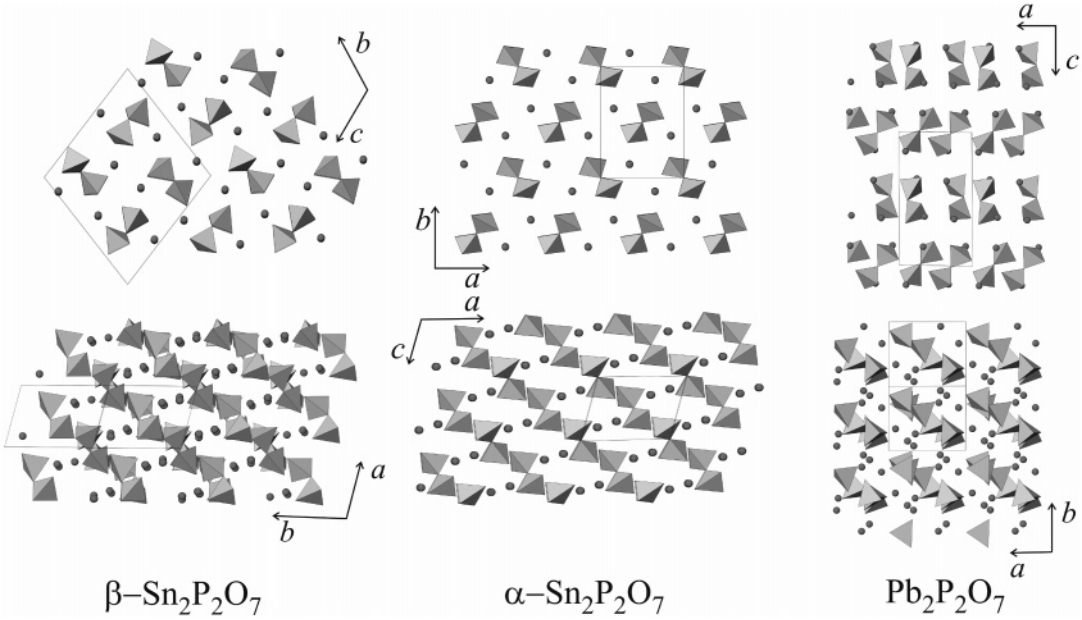

Figure 10. Comparison of crystal structures for two modifications of $Sn_2P_2O_7$ with the structure of $Pb_2P_2O_7$.

should be noted, however, that the mutually perpendicular placement of the P_2O_7 groups does not necessarily result in the formation of large structural interstices. For example, a similar orientation of such groups was found in the SnP_2O_7 compound,[17] which nevertheless exhibits a structure similar to a close packed cubic one.

As was mentioned before, based on the similarities of the XRPD patterns, the crystal structures of both the LT and HT modifications are closely related. Projections for the LT and HT structures (Figure 10) illustrate this statement. Two upper projections (along the [100] and [001] axes for β- and α-modifications, respectively) exhibit horizontal "rows" of P_2O_7 units. These groups are similarly oriented within the same row, but are perpendicular to the groups in neighboring rows. The phase transition does not affect this ordering. The main change during the phase transformation from LT to HT form results, as can be seen from Figure 10, only in an alteration of the geometry of the P_2O_7 groups, which become more symmetrical due to the appearance of an inversion center at the bridging O(1) atom in the HT structure. The distribution of tin atoms remains almost unchanged. Presented projections of the two crystal structures allow us to deduce a transformation matrix from β- to α- form as:

$$\begin{pmatrix} 0 & -1/2 & -1/2 \\ 0 & 1/2 & -1/2 \\ -1 & 0 & 0 \end{pmatrix}, \det = \frac{1}{2}$$

The determinant of the matrix indicates a twice larger cell volume for β-modification as was found in the experiment.

The crystal structure of $Pb_2P_2O_7$[18] can be considered as closely related to that of $Sn_2P_2O_7$ (Figure 10). The Pb^{2+} cation also possesses a lone electron pair, therefore, the pyrophosphate groups in the adjacent "rows" of the $Pb_2P_2O_7$ structure (see the $a-c$ projection) are not parallel to each other although they are still not perpendicular as was found for the tin containing compound (see, for instance, the $a-b$ projection for α-$Sn_2P_2O_7$). In the same "row" the pyrophosphate groups appear by pairs. This leads to noticeably different distribution of Pb^{2+} cations in the unit cell as compared to the distribution of tin ions in the $Sn_2P_2O_7$ structures. This difference is clearly seen in Figure 10 for the Pb^{2+} ions located between "layers" of pyrogroups (the $a-b$ projection).

In conclusion, the highly asymmetric valence electron distribution in Sn^{2+} or Pb^{2+} cations induces a significant change in the structure of their pyrophosphates in comparison with other $M_2P_2O_7$ divalent metal compounds. The high-temperature transition in the $Sn_2P_2O_7$ is obviously induced by transformation of the distorted pyrophosphate groups to more symmetrical structural units.

Acknowledgment. We are grateful to RFBR (grant 04-03-32787) and ICDD (GiA APS91-05) for financial support. We thank Dr. M. Kovba for his assistance with synthetic procedures, Dr. M. Zhizhin for high-temperature XRPD data collection, and Drs. T. Smirnova and I. Arkhangelsky for help with thermal analysis experiments. E.D. thanks the National Science Foundation (NSF-CHE-01300985).

Supporting Information Available: Crystallographic information (cif). This material is available free of charge via the Internet at http://pubs.acs.org.

CM048463H

(17) Huang, C. H.; Knop, O.; Othen, D. A.; Woodhams, F. W. D.; Howie, R. A.; *Can. J. Chem.* **1975**, *53*, 79−91.

(18) Mullica, D. F.; Perkins, H. O.; Grossie, D. A.; Boatner, L. A.; Sales, B. C. *J. Solid State Chem.* **1986**, *62*, 371−376.